Purification and Many-Body Localization in Cold Atomic Gases

Felix Andraschko,[1,2] Tilman Enss,[3] and Jesko Sirker[1,2]
[1]Department of Physics and Research Center OPTIMAS, Technical University Kaiserslautern, D-67663 Kaiserslautern, Germany
[2]Department of Physics and Astronomy, University of Manitoba, Winnipeg R3T 2N2, Canada
[3]Institut für Theoretische Physik, Universität Heidelberg, D-69120 Heidelberg, Germany
(Received 16 July 2014; revised manuscript received 19 August 2014; published 17 November 2014)

We propose to observe many-body localization in cold atomic gases by realizing a Bose-Hubbard chain with binary disorder and studying its nonequilibrium dynamics. In particular, we show that measuring the difference in occupation between even and odd sites, starting from a prepared density-wave state, provides clear signatures of localization. Furthermore, we confirm as hallmarks of the many-body localized phase a logarithmic increase of the entanglement entropy in time and Poissonian level statistics. Our numerical density-matrix renormalization group calculations for infinite system size are based on a purification approach; this allows us to perform the disorder average exactly, thus producing data without any statistical noise and with maximal simulation times of up to a factor 10 longer than in the clean case.

DOI: 10.1103/PhysRevLett.113.217201 PACS numbers: 75.10.Jm, 05.70.Ln, 72.15.Rn

Cold atomic gases with or without optical lattices are an ideal platform to realize model Hamiltonians of strongly correlated quantum systems by offering an unprecedented control over the microscopic parameters [1]. Among the many achievements are the observation of the superfluid-to-Mott-insulator transition for a Bose gas held in a three-dimensional optical lattice [2], the realization of the Tonks-Girardeau regime in a quasi-one-dimensional (1D) Bose gas [3], and the simulation of the nonequilibrium dynamics in an almost-integrable one-dimensional quantum system [4].

While these experiments have all been performed on very clean systems, there is also a tremendous interest in building quantum simulators for models with disorder. This interest is sparked by the unavoidable presence of disorder and impurities in real materials that can lead to completely new physics, such as the Kondo effect and Anderson localization [5]. For cold atomic gases there have been several different approaches to realize disorder. The first experiments have employed quasiperiodic lattices or laser speckles to study Anderson localization in effectively noninteracting Bose condensates in one and three dimensions [6]. As an alternative it has been suggested to use the repulsive interactions between two different species of atoms—with one being effectively immobile—to obtain a binary disorder potential for the mobile species on the scale of the lattice constant [7,8]. Experimentally, the localization of bosonic atoms by fermionic impurities has been demonstrated [9].

Theoretically, it has been suggested by Anderson [5] that a localized phase might be stable against small interactions, a result which has been supported by a recent study [10] leading to a renewed interest in many-body localization (MBL). In interacting spin chains with a random magnetic field drawn from a box distribution, in particular, a transition is found between a delocalized, ergodic phase at weak disorder and a many-body localized phase at strong disorder [11–13]. In a MBL phase, where all many-body eigenstates are localized, a simple picture emerges: In this case one can separate a chain [14] into segments of length $\ell \gg \xi$, where ξ is the localization length. The many-body eigenstates of the whole chain are then, to a good approximation, product states of the eigenstates in each segment. Importantly, projectors onto the eigenstates of a segment are local conserved charges with finite support and have to be included in a generalized Gibbs ensemble [15]. This constrains the dynamics and prevents thermalization in any subsystem [16,17]. Residual interactions between segments make these charges quasilocal; i.e., contributions to the conserved charge with spatial support on any length scale r exist, but are suppressed as $\exp(-r)$. The conserved charges thus remain relevant for transport and nonequilibrium dynamics [18]. The residual long-range interactions are also responsible for the observed growth of the entanglement entropy, $S \sim \ln t$, with time t if the system is prepared in a product state and evolves in time [16,19,20]. This is one of the hallmarks of a MBL phase, in contrast to the linear growth in systems without disorder [21] and the extremely slow increase, $S \sim \ln\ln t$, found for a noninteracting model with bond disorder [22]. Experimentally, however, this new state of matter has not yet been detected, and the question of which kind of system and which local observables are appropriate for this purpose is considered as one of the main open problems in this field [23].

In this Letter we discuss the possible realization and observation of many-body localization in a system of cold atoms. Consider two interacting species of bosons in an optical lattice, with one of them frozen to form a binary disorder potential for the other, mobile species [7,8]. The effective Hamiltonian for the mobile bosons is

$$H = -(J/2)\sum_j (a_j^\dagger a_{j+1} + \text{H.c.}) + \sum_j [U n_j(n_j-1)/2 + V n_j n_{j+1} + J D_j n_j], \quad (1)$$

where J is the hopping amplitude, $n_j = a_j^\dagger a_j$ the local density, U the onsite interaction, and V the nearest-neighbor interaction. The effective binary disorder potential D_j is drawn randomly according to $D_j = \pm D$, and we have neglected the trapping potential. We consider in the following the case where the mobile species is prepared in the initial density-wave state $|\Psi_0\rangle = |010101\cdots\rangle$. During the ensuing time evolution under the Hamiltonian (1) we propose to measure the difference in occupation between the even and odd sites, $\Delta n = N^{-1}\sum_j (-1)^j(\langle n_j\rangle - 1/2)$, where N is the number of lattice sites. Exactly this setup has already been realized in the clean case, i.e., for a single species of bosons [24]. By freezing the immobile bosons into a quantum state which is close to an equal superposition of Fock states $|n_1, n_2, \cdots\rangle$ with $n_j \in \{0, 1\}$, the time-evolved state is automatically averaged over all binary disorder configurations [8,25]. This purification method can also be used for numerical computations and is explained in detail below. Our proposal thus combines realizing disorder in optical lattices using two species of atoms [9] with techniques to prepare initial states and to measure their nonequilibrium dynamics [24]. Experimentally, this can be realized, for instance, with two hyperfine states of ^{87}Rb atoms loaded into a state-dependent optical lattice: The wavelength controls the relative hopping amplitude of both states, while the intraspecies interaction is tuned by a Feshbach resonance, and the interspecies interaction depends on the intensity of the laser beam. In this way, both the ratio of onsite interaction U to hopping amplitude J and the coupling between mobile and disorder atoms can be tuned independently, and bimodal disorder with very short-range correlations is realized [8].

Let us first discuss the cases $V = 0$ with $U = 0$ or $U = \infty$ with strong disorder $D \gg 1$. In this case, each disorder configuration splits the chain into segments of equal potential D_i, which communicate very little with their neighboring segments due to the mismatch of the local potential energy and the kinetic energy, $JD \gg J$: For a given segment, Δn has contributions from neighboring segments of the order of $1/D^2$. Thus, the segments become isolated in the limit $D \to \infty$. The time evolution of the whole chain is then given by summing up the independent time evolution of open segments $\Delta n^{(\ell)}(t)$ of varying length ℓ, weighted by their probability of occurrence, $p_\ell = \ell/2^{\ell+1}$ with $\sum_\ell p_\ell = 1$, leading to $\Delta n^{D=\infty}(t) = \sum_{\ell=1}^\infty p_\ell \Delta n^{(\ell)}(t)$ both for $U = 0$ and $U = \infty$ [26]. It is easy to see that only segments of odd chain length contribute to the long-time average with $\overline{\Delta n}^{(\ell)}_{\text{odd}} = 1/(2\ell)$, so that $\overline{\Delta n} = \sum_\ell p_\ell \overline{\Delta n}^{(\ell)} = \frac{1}{2}\sum_{\ell\,\text{odd}} p_\ell/\ell = \frac{1}{6}$.

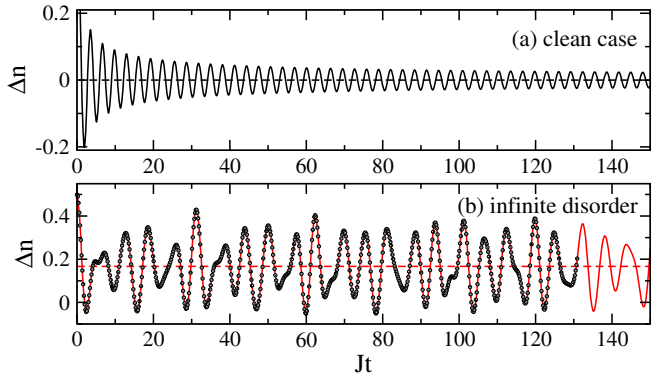

FIG. 1 (color online). $\Delta n(t)$ for model (1) with $V = 0$ and $U = 0$ or $U = \infty$: (a) $\Delta n^{D=0}$ vs (b) $\Delta n^{D=\infty}$ (solid red) with average $\overline{\Delta n} = 1/6$ (dashed red); symbols are light-cone renormalization group (LCRG) results.

Figure 1(a) shows the time evolution in the clean case, where for both $U = 0$ and $U = \infty$ one finds $\Delta n^{D=0}(t) = J_0(2Jt)/2$, with the Bessel function $J_0(x)$ [27,28]. In comparison, the time evolution in the strongly disordered case, Fig. 1(b), appears very complicated. Yet, including only segments up to a maximum length L already gives an approximation with an exponentially small error $\sim L/2^L$ at all times, because p_ℓ decays exponentially.

Model (1) is difficult to treat numerically because of the unrestricted local Hilbert-space dimension for finite interaction strength U. We will therefore first concentrate on the limit $U \to \infty$, where numerical methods are very efficient. We will firmly establish that a MBL phase exists in this limit before returning to the case of finite U at the end of this Letter. For $U \to \infty$, the above model maps onto the spin-1/2 XXZ chain

$$H = -J\sum_i (s_i^x s_{i+1}^x + s_i^y s_{i+1}^y - \Delta s_i^z s_{i+1}^z - D_i s_i^z), \quad (2)$$

with anisotropy $J\Delta = V$ [29]. $|\Psi_0\rangle$ is then the Néel state and $\Delta n = N^{-1}\sum_j (-1)^j \langle s_j^z\rangle$ is the staggered magnetization. For $\Delta = 0$, the dynamics is again given by Fig. 1(a) in the clean case and by Fig. 1(b) in the strongly disordered case. For alkali atoms, $V \ll J$, so that a realization of the XXZ model with substantial Δ is not easily achievable. We note, though, that the isotropic Heisenberg chain, $\Delta = 1$, has recently been realized using two boson species, and that the nonequilibrium dynamics has been studied with single-site addressability [30]. Furthermore, longer-range interactions are also present if dipolar gases or polar molecules are used [31].

To simulate the nonequilibrium dynamics of the Bose-Hubbard model (1) and the XXZ model (2) for all interaction and disorder strengths, and to perform an exact disorder average, we use the light-cone renormalization group (LCRG) [28]. The LCRG algorithm is a variant of the density-matrix renormalization group (DMRG) technique [32] based on the Lieb-Robinson bounds [33]:

A local measurement at time t is affected only by the degrees of freedom within its light cone. The opening angle of the light cone, or spreading velocity, is determined by model parameters. For lattice models with short-range interactions, the time evolution operator $\mathcal{U} = \exp(-iHt)$ has a Trotter-Suzuki decomposition with a checkerboard structure: Within the LCRG, a light cone out of the infinite checkerboard is sufficient to compute the time evolution of local observables in an infinite system [28,34].

To treat disorder, one straightforward possibility for a finite system is to compute the time evolution for one particular disorder configuration, and then repeat the calculation for many different configurations to obtain the disorder average. Here, we instead use purification for an infinite system in order to perform the full disorder average in a single run [25], at the expense of enlarging the Hilbert space. Specifically, for the XXZ chain, an ancilla spin-1/2, $\vec{s}_{i,\mathrm{anc}}$, is added to each lattice site with an Ising coupling, $D_i s_i^z \mapsto 2D s_i^z s_{i,\mathrm{anc}}^z$. The state of $s_{i,\mathrm{anc}}^z = \pm 1/2$ now determines the local Zeeman field $D_i = \pm D$. There is no coupling between different ancilla spins; hence, they have no dynamics and represent static disorder. The time evolution of the disorder average is given by the evolution from a prepared product state $|\psi_0\rangle \otimes |\mathrm{dis}\rangle$ in the enlarged Hilbert space of spins and ancillas, where $|\mathrm{dis}\rangle = \bigotimes_j (|\uparrow\rangle_j + |\downarrow\rangle_j)/\sqrt{2}$ is the fully mixed state for the ancillas. The disorder-averaged expectation value of an operator O is then obtained by measuring the expectation value of the operator $O \otimes \mathbb{1}_{\mathrm{anc}}$ in the enlarged Hilbert space. Although the local Hilbert-space dimension is doubled, the LCRG algorithm works even more efficiently for strongly disordered systems than for clean systems, and real times up to $Jt \sim 100$ are reached in our simulations, where we keep the truncation error in each renormalization group step smaller than 10^{-8} by dynamically increasing the number of kept states up to 20 000. Responsible for these long simulation times is the slow logarithmic growth of the entanglement entropy, S_{ent}, for $\Delta \neq 0$, see Fig. 2. Here, $S_{\mathrm{ent}} = -\mathrm{Tr}\rho_B \ln \rho_B$, where ρ_B is the reduced density matrix obtained by cutting the infinite chain, $A \otimes B$, of spins *and* ancillas in half. Since entanglement in the static ancillas is mediated by the spins, S_{ent} has the same functional dependence on time as the disorder-averaged entanglement entropy of a spin-only system [26]. The logarithmic increase for $\Delta \neq 0$ is the same behavior as seen for the XXZ model with the magnetic fields D_i drawn from a box distribution [20], and is a hallmark of a MBL phase. On the other hand, S_{ent} saturates for $\Delta = 0$ and infinite binary disorder, see the inset of Fig. 2. The latter behavior can be easily understood by noting that S_{ent} for a block of size $n \leq \ell$ of a finite chain segment of spins and ancillas with length ℓ is bounded, $S_{\mathrm{ent}} \leq n \ln 4$. Since p_ℓ decreases exponentially, a strict bound for S_{ent} at all times exists [26]. This is different from the case of strong bond disorder, where $S_{\mathrm{ent}} \sim \ln\ln t$ [22].

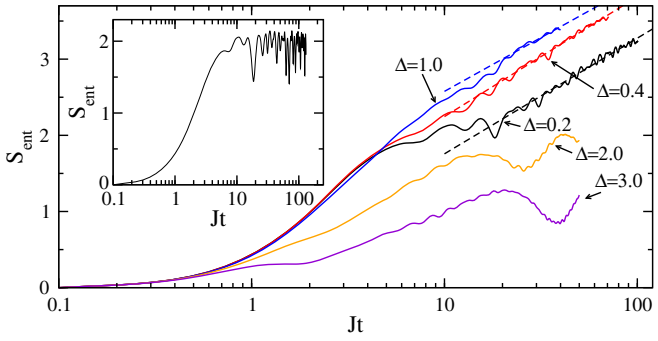

FIG. 2 (color online). S_{ent} for the XXZ chain (2) in the strongly disordered case $D = 4000$. For small Δ we find asymptotically $S_{\mathrm{ent}}(t) \sim \ln t$ (dashed lines are fits for $t > 20$). Inset: $S_{\mathrm{ent}}(t)$ saturates for $\Delta = 0$ and infinite disorder.

In Figs. 3(a) and 3(b) we show $\Delta n(t)$ for strong and intermediate disorder. In all cases shown, $\Delta n(t)$ does not decay to zero, indicating that the system does not thermalize. The strong reduction of the variance of $\Delta n(t)$ with increasing Δ [see Fig. 3(c)] is a clear experimental indication that localization in an interacting system is observed.

To further support our findings of a MBL phase for the XXZ model with binary disorder, we have also calculated the level statistics for finite chains of up to $N = 14$ sites in the $S^z = 0$ sector by exact diagonalization of all 2^N possible disorder realizations. In the integrable XXZ chain without disorder, a full set of local integrals of motion exists, which allows us to completely classify the eigenvalues by the corresponding quantum numbers. The spectrum is therefore uncorrelated and the corresponding level statistics Poissonian, $\mathcal{P}(s) = \exp(-s)$, in terms of the level spacing s. Disorder breaks integrability, so that the level-spacing distribution, if the many-body states are extended, will follow a Wigner distribution, $\mathcal{P}(s) = (\pi s/2)\exp(-\pi s^2/4)$. This can also be understood as a crossover from integrability to quantum chaos [35]. However, once localization sets in,

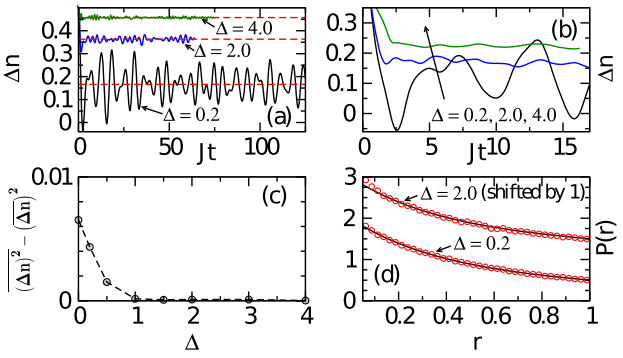

FIG. 3 (color online). XXZ chain: (a) $\Delta n(t)$ for $D = 4000$ with averages (dashed lines). $D = 1.5$: (b) $\Delta n(t)$, (c) variance of $\Delta n(t)$ for $t > 5$, and (d) $P(r)$ for chains of length $N = 14$ (symbols) and $P(r) = 2/(1+r)^2$ (solid lines).

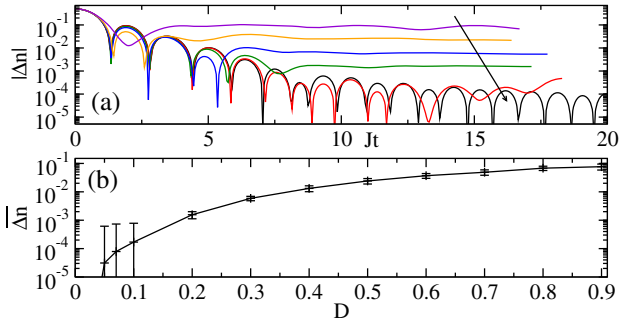

FIG. 4 (color online). (a) $\Delta n(t)$ for the Heisenberg point, $\Delta = 1$, and disorder strengths $D = 0.9, 0.5, 0.3, 0.2, 0.1, 0.0$ (in arrow direction). (b) $\overline{\Delta n}$ obtained by averaging over intervals $[t_{\min}, 20]$ with $t_{\min} > 5$ variable (see error bars).

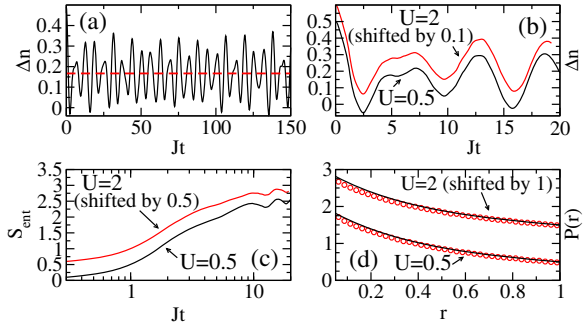

FIG. 5 (color online). Bose-Hubbard model with $V = 0$. (a) $\Delta n(t)$ for $D = \infty$ and $U = 2$ with average (dashed line). Disorder strength $D = 6$: (b) $\Delta n(t)$, (c) $S_{\text{ent}}(t)$, and (d) $P(r)$ for $N = 14$ (symbols) and $P(r) = 2/(1 + r)^2$ (solid lines).

the spectrum will again become uncorrelated, because localization creates new quasi-local conserved charges, leading to a Poissonian level statistics. In this case chaos is incomplete and the system keeps a memory of the initial state [35]. If a critical $D_c \neq 0$ for localization exists, we therefore expect to go from a Poissonian ($D = 0$, integrable) to a Wigner distribution ($0 < D < D_c$, nonintegrable and delocalized), and then again back to a Poissonian ($D > D_c$, localized) [26]. Here, we concentrate on the regime far from the clean integrable limit. In order to avoid the ambiguous definition of an average gap based on a construction of a continuous density of states from finite-size data, we consider the ratio r between two consecutive gaps of adjacent energy levels as defined in Refs. [11,12]. If the level statistics is Poissonian, the distribution function of gap ratios $0 \leq r \leq 1$ is given by $P(r) = 2/(1 + r)^2$. As shown in Fig. 3(d), this is in good agreement with the numerical results [26].

Of particular interest is the isotropic Heisenberg chain, $\Delta = 1$, which has recently been realized in cold atomic gases [30] and approximately describes materials such as Sr_2CuO_3 and $SrCuO_2$ [36]. In the latter case, a doping with nonmagnetic impurities, such as Pd, is possible, which randomly replace the magnetic Cu^{2+} ions [37]. As in model (2), for strong disorder, the chain then separates into segments; however, the coupling between the segment ends is now not an Ising, but a Heisenberg coupling caused by next-nearest-neighbor interactions [38]. In such systems, many-body localization should also occur, preventing local excitations from spreading. However, phonons complicate the observation of MBL, leaving cold atomic gases as a particularly clean and promising realization. In Fig. 4, results for the Heisenberg model with binary disorder are shown. Here, clear signatures for MBL are already seen for small disorder, with $\Delta n(t)$ quickly approaching a nonzero constant value, see Fig. 4(a), while $\Delta n(t)$ decays completely in the clean case [27]. By averaging over different time intervals, we can extract an estimate for the long-time average $\overline{\Delta n}$ with error bounds, see Fig. 4(b). The results are consistent with a critical value D_c for the localization transition which is either zero or finite, but with $D_c < 0.2$. A detailed analysis of the phase diagram, including the crossover from integrable to (incomplete) chaotic behavior, will be presented elsewhere [39].

Let us finally return to the full Bose-Hubbard model (1), which we have proposed to realize experimentally. We concentrate on the case of vanishing nearest-neighbor interaction, $V = 0$, realized in alkali atoms. For infinite disorder strength, the system still separates into decoupled chain segments for any interaction strength U. In this case, we can simulate the dynamics for arbitrary times by exactly diagonalizing the segments, see Fig. 5(a). Note that in the limit $D \to \infty$, $S_{\text{ent}}(t)$ is bounded: There is no many-body localization in this case. At finite disorder, we again use the LCRG algorithm to simulate the system. Results for $\Delta n(t)$ and $S_{\text{ent}}(t)$ are shown in Figs. 5(b) and 5(c), respectively. Although the simulation time is more limited than in the XXZ case, $\Delta n(t)$ seems to remain nonzero, while the data for S_{ent} are consistent with a logarithmic increase, as expected in a MBL phase. This is corroborated further by the distribution function of gap ratios $P(r)$, see Fig. 5, consistent with a Poissonian level statistics.

To conclude, we have proposed to study many-body localization in cold atomic gases by realizing a Bose-Hubbard model with binary disorder provided by a second species, and studying its quench dynamics. Both experimentally as well as in numerical calculations, one can make use of purification to achieve an automatic disorder average. By implementing the purification scheme into a DMRG algorithm, we have shown that the nonequilibrium dynamics can be simulated in a single run without any stochastic noise, and with simulation times for strong disorder that are significantly longer than in the clean case, making DMRG-type algorithms an ideal tool to investigate infinite, disordered systems. Both in the Bose-Hubbard model as well as in the XXZ chain limit, we have shown that a MBL phase exists and can be detected by measuring the one-point function $\Delta n(t)$.

F. A. and J. S. acknowledge support by the Collaborative Research Centre SFB/TR49, the Graduate School of Excellence MAINZ (DFG, Germany), as well as NSERC (Canada). We are grateful to the Regional Computing Center at the University of Kaiserslautern, the AHRP, and Compute Canada for providing computational resources and support.

[1] I. Bloch, J. Dalibard, and W. Zwerger, Rev. Mod. Phys. **80**, 885 (2008).
[2] M. Greiner, O. Mandel, T. Esslinger, T. W. Hänsch, and I. Bloch, Nature (London) **415**, 39 (2002).
[3] B. Paredes, A. Widera, V. Murg, O. Mandel, S. Fölling, I. Cirac, G. V. Shlyapnikov, T. W. Hänsch, and I. Bloch, Nature (London) **429**, 277 (2004).
[4] T. Kinoshita, T. Wenger, and D. S. Weiss, Nature (London) **440**, 900 (2006).
[5] P. W. Anderson, Phys. Rev. **109**, 1492 (1958).
[6] G. Roati, C. D'Errico, L. Fallani, M. Fattori, C. Fort, M. Zaccanti, G. Modugno, M. Modugno, and M. Inguscio, Nature (London) **453**, 895 (2008); J. Billy, V. Josse, Z. Zuo, A. Bernard, B. Hambrecht, P. Lugan, D. Clément, L. Sanchez-Palencia, P. Bouyer, and A. Aspect, Nature (London) **453**, 891 (2008); M. White, M. Pasienski, D. McKay, S. Q. Zhou, D. Ceperley, and B. DeMarco, Phys. Rev. Lett. **102**, 055301 (2009); F. Jendrzejewski, A. Bernard, K. Müller, P. Cheinet, V. Josse, M. Piraud, L. Pezzé, L. Sanchez-Palencia, A. Aspect, and P. Bouyer, Nat. Phys. **8**, 398 (2012).
[7] U. Gavish and Y. Castin, Phys. Rev. Lett. **95**, 020401 (2005); T. Roscilde and J. I. Cirac, Phys. Rev. Lett. **98**, 190402 (2007); S. Morrison, A. Kantian, A. J. Daley, H. G. Katzgraber, M. Lewenstein, H. P. Büchler, and P. Zoller, New J. Phys. **10**, 073032 (2008).
[8] B. Horstmann, J. I. Cirac, and T. Roscilde, Phys. Rev. A **76**, 043625 (2007); B. Horstmann, S. Dürr, and T. Roscilde, Phys. Rev. Lett. **105**, 160402 (2010).
[9] S. Ospelkaus, C. Ospelkaus, O. Wille, M. Succo, P. Ernst, K. Sengstock, and K. Bongs, Phys. Rev. Lett. **96**, 180403 (2006).
[10] D. M. Basko, I. L. Aleiner, and B. L. Altshuler, Ann. Phys. (Amsterdam) **321**, 1126 (2006).
[11] V. Oganesyan and D. A. Huse, Phys. Rev. B **75**, 155111 (2007).
[12] A. Pal and D. A. Huse, Phys. Rev. B **82**, 174411 (2010).
[13] C. Monthus and T. Garel, Phys. Rev. B **81**, 134202 (2010); E. Canovi, D. Rossini, R. Fazio, G. E. Santoro, and A. Silva, Phys. Rev. B **83**, 094431 (2011); J. Z. Imbrie, arXiv:1403.7837; T. Grover, arXiv:1405.1471.
[14] We concentrate here on the one-dimensional case, but the argument is general and also applicable in higher dimensions.
[15] M. Rigol, V. Dunjko, V. Yurovsky, and M. Olshanii, Phys. Rev. Lett. **98**, 050405 (2007).
[16] R. Vosk and E. Altman, Phys. Rev. Lett. **110**, 067204 (2013).
[17] C. Gogolin, M. P. Müller, and J. Eisert, Phys. Rev. Lett. **106**, 040401 (2011); G. Carleo, F. Becca, M. Schiró, and M. Fabrizio, Sci. Rep. **2**, 243 (2012); M. Serbyn, Z. Papić, and D. A. Abanin, Phys. Rev. Lett. **111**, 127201 (2013); D. A. Huse and V. Oganesyan, arXiv:1305.4915; Y. Bar Lev and D. R. Reichman, Phys. Rev. B **89**, 220201(R) (2014); R. Vasseur, S. A. Parameswaran, and J. E. Moore, arXiv:1407.4476.
[18] T. Prosen, Phys. Rev. Lett. **106**, 217206 (2011); J. Sirker, N. P. Konstantinidis, F. Andraschko, and N. Sedlmayr, Phys. Rev. A **89**, 042104 (2014).
[19] G. De Chiara, S. Montangero, P. Calabrese, and R. Fazio, J. Stat. Mech. (2006) P03001; M. Žnidarič, T. Prosen, and P. Prelovšek, Phys. Rev. B **77**, 064426 (2008); R. Vosk and E. Altman, Phys. Rev. Lett. **112**, 217204 (2014); A. Nanduri, H. Kim, and D. A. Huse, Phys. Rev. B **90**, 064201 (2014); M. Serbyn, M. Knap, S. Gopalakrishnan, Z. Papić, N. Y. Yao, C. R. Laumann, D. A. Abanin, M. D. Lukin, and E. A. Demler, Phys. Rev. Lett. **113**, 147204 (2014).
[20] J. H. Bardarson, F. Pollmann, and J. E. Moore, Phys. Rev. Lett. **109**, 017202 (2012).
[21] S. Bravyi, M. B. Hastings, and F. Verstraete, Phys. Rev. Lett. **97**, 050401 (2006).
[22] F. Iglói, Z. Szatmári, and Y.-C. Lin, Phys. Rev. B **85**, 094417 (2012).
[23] E. Altman and R. Vosk, arXiv:1408.2834.
[24] S. Trotzky, Y.-A. Chen, A. Flesch, I. P. McCulloch, U. Schollwöck, J. Eisert, and I. Bloch, Nat. Phys. **8**, 325 (2012).
[25] B. Paredes, F. Verstraete, and J. I. Cirac, Phys. Rev. Lett. **95**, 140501 (2005).
[26] See Supplemental Material at http://link.aps.org/supplemental/10.1103/PhysRevLett.113.217201 for details.
[27] P. Barmettler, M. Punk, V. Gritsev, E. Demler, and E. Altman, Phys. Rev. Lett. **102**, 130603 (2009); New J. Phys. **12**, 055017 (2010).
[28] T. Enss and J. Sirker, New J. Phys. **14**, 023008 (2012).
[29] D. Giuliano, D. Rossini, P. Sodano, and A. Trombettoni, Phys. Rev. B **87**, 035104 (2013).
[30] T. Fukuhara *et al.*, Nat. Phys. **9**, 235 (2013).
[31] N. Y. Yao *et al.*, arXiv:1311.7151; K. R. A. Hazzard *et al.*, arXiv:1406.0937.
[32] S. R. White, Phys. Rev. Lett. **69**, 2863 (1992); A. J. Daley *et al.*, J. Stat. Mech. (2004) P04005; S. R. White and A. E. Feiguin, Phys. Rev. Lett. **93**, 076401 (2004).
[33] E. H. Lieb and D. W. Robinson, Commun. Math. Phys. **28**, 251 (1972).
[34] F. Andraschko and J. Sirker, Phys. Rev. B **89**, 125120 (2014).
[35] V. A. Yurovsky and M. Olshanii, Phys. Rev. Lett. **106**, 025303 (2011).
[36] N. Motoyama, H. Eisaki, and S. Uchida, Phys. Rev. Lett. **76**, 3212 (1996).
[37] K. M. Kojima *et al.*, Phys. Rev. B **70**, 094402 (2004).
[38] J. Sirker, N. Laflorencie, S. Fujimoto, S. Eggert, and I. Affleck, Phys. Rev. Lett. **98**, 137205 (2007); J. Stat. Mech. (2008) P02015.
[39] T. Enss, F. Andraschko, and J. Sirker (to be published).